

Imaging and Photometry

Brightness



- Probably the most fundamental property any astronomical object is its energy output
 - Provides information on energy source and scale
- By measuring the brightness of an object, we can calculate the energy output
 - Providing we know how far away it
 - and we correct it for any energy loss
 - providing the output is isotropic
 - and we can measure the total brightness, i.e. across the full spectrum (and account for any other energy loss such as neutrinos)
 - Or for known object classes, accurate photometry may indicate distances
- To do this accurately, we have to calibrate our measurements carefully and turn them into useful numbers – and that is where the trouble starts.....
- Unfortunately different wavebands use different measures of brightness

Magnitudes

- Historic brightness scale :
 - mag 1 is bright and 6 is the faintest visible to the eye
 - brightest star at V: Sirius has $m_V = -1.4$,
 - HST limit is $\sim 31^{\text{st}}$ magnitude, $\sim 10^{13}$ times fainter than Sirius
- Logarithmic scale, 5 mag \equiv factor of 100
 - proposed by Norman Pogson of the Radcliffe Observatory (1856)
- Standard photometric systems based on photoelectric measurements made in the 1960s (Johnson - UBVRI):
 - U is shortward of Balmer discontinuity
 - B is peak of photographic plate response
 - V is peak of human eye response
- Vega (Spectral type A0, $T \sim 10^4 \text{K}$) has mag=0 in all bands
- Other stars are then measured with respect to this star – fundamental calibrator

Types of Magnitude

- *Apparent* - m - measured magnitude relative to Vega or other fundamental calibrators in a defined passband, e.g. m_V
- *Absolute* - M - the apparent magnitude the object would have if it were at a distance of 10pc. So a measure of the total output within the band
- *Bolometric* - M_{bol} is the bolometric magnitude of the star given by
$$M_{\text{bol}} = -2.5 \text{ Log}_{10} (L_*/L_0)$$
 L_* (the star's luminosity in Watts) is relative to an object with a luminosity of $L_0 = 3.0128 \times 10^{28}$ W across the whole electromagnetic spectrum (the IAU-decreed luminosity for $M_{\text{bol}} = 0.0$)
- The bolometric magnitude of the sun is $M_{\text{bol}} = 4.74$
- Note $M_{\text{bol}} = M_V - \text{BC}$ - the Bolometric Correction which accounts for the emission outside the V passband
- In practice, may also need to account for interstellar extinction (A_V) so that $M_{\text{bol}} = M_V - \text{BC} - A(V)$

Distance Modulus

A measure of the distance expressed as the difference between the apparent magnitude of object compared to what it would be at a distance of 10pc : $\mu = m - M$

$$\text{Log}_{10} (d) = 1 + \mu / 5, \quad \text{with } d \text{ in pc}$$

$$(m - M)_V = 5 \times \log (D/10\text{pc})$$

e.g. the distance modulus to the LMC (50kpc) = 18.5



Vega magnitudes work well for stellar photometry as the colours from pairs of filters indicate stellar temperatures

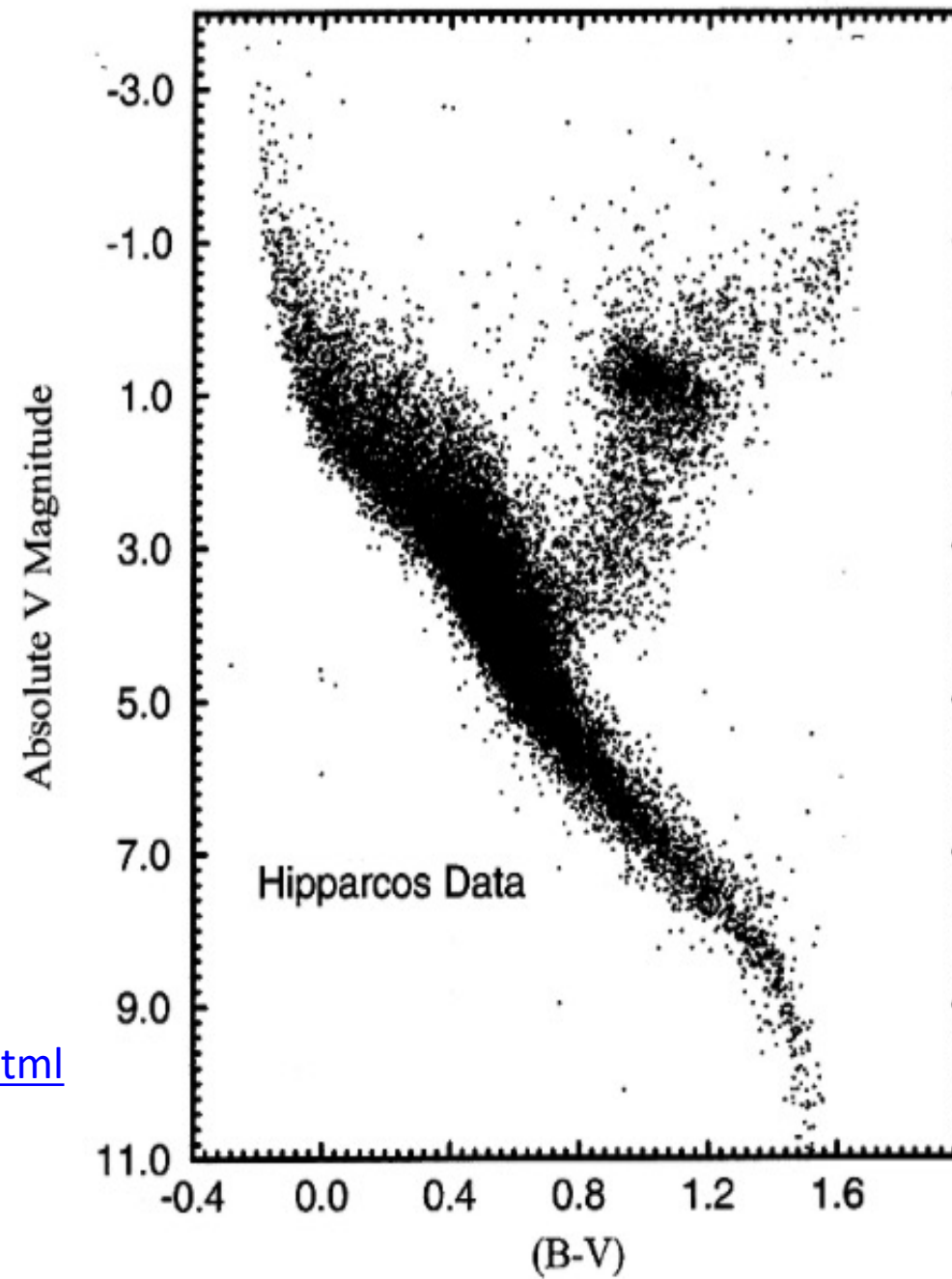
Different Photometric systems use different filters; e.g. **Stromgren** (narrow band filters used to estimate T, g, metallicity)

AB magnitudes :

Source with constant flux per unit freq. has zero colour. With flux measured in $\text{erg s}^{-1} \text{cm}^{-2} \text{Hz}^{-1}$
 $m_{\text{AB}} = -2.5 \log(f) - 48.60$

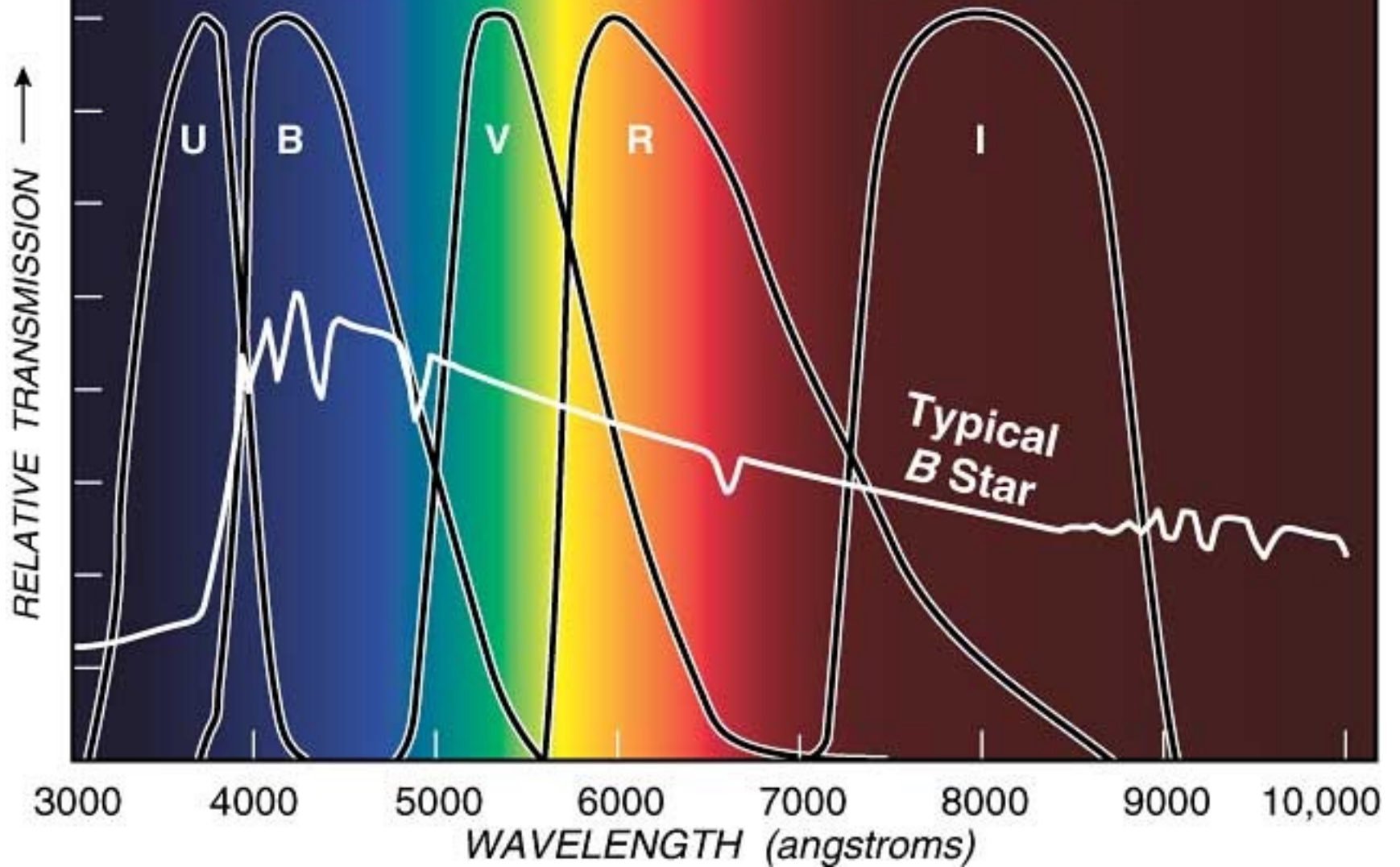
Sloan u'g'r'i'z' system similar to AB
<http://classic.sdss.org/dr4/algorithms/fluxcal.html>

STMAG (Space Telescope magnitude system) Source with constant flux per unit wavelength has zero colour



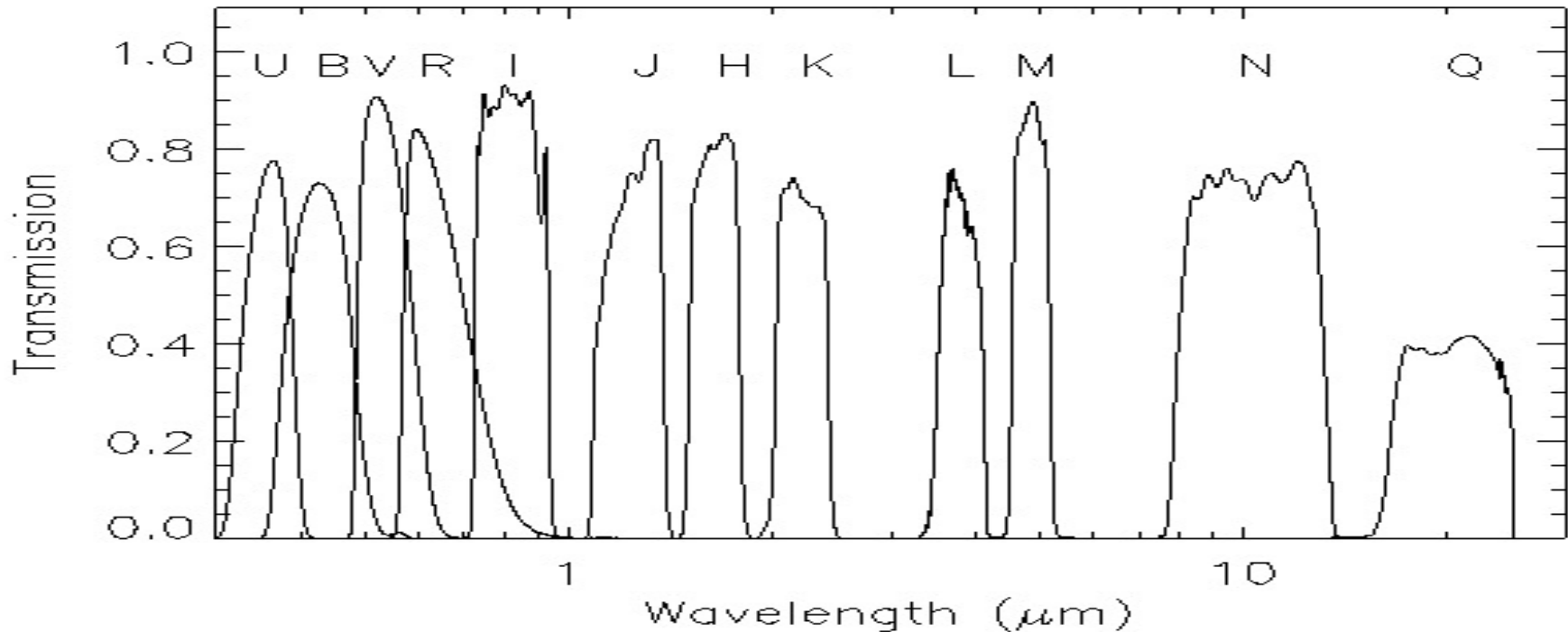
2. Color-Absolute Magnitude diagram for the nearby stars measured by the Hipparcos-Tycho s

Standard Photometric Filters

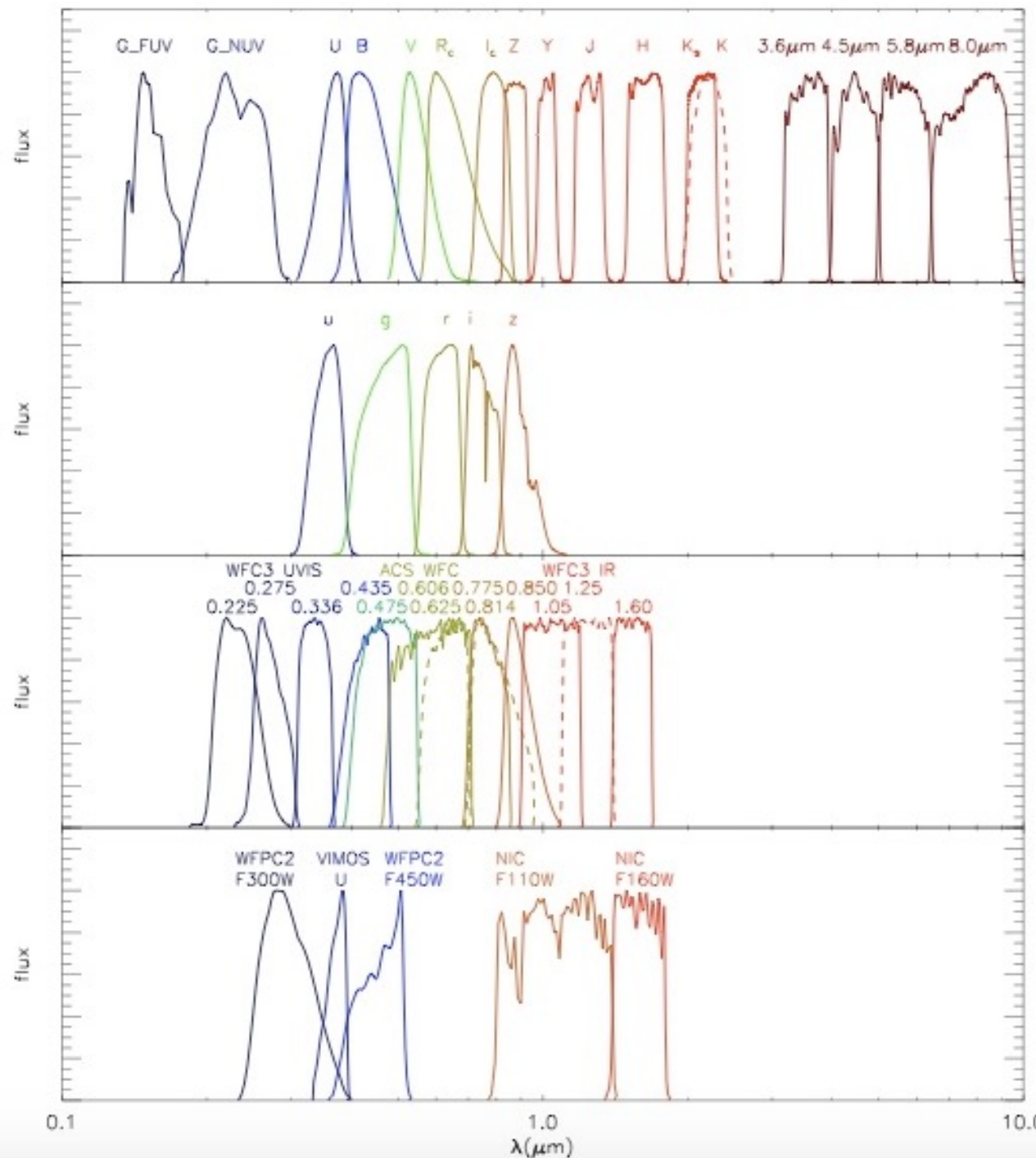


Extension to IR

- UBVRIJHKLMNQ 0.3 to 25 μm
 - Additional filters : Z \sim 0.88 μm , Y \sim 1.02 μm
 - IR filters match the atmospheric windows for ground-based observations.
 - Satellites have more options



- Comparison of different filter profiles:
- Top GALEX FUV and NUV, Johnson-Bessel U, B, V, Cousins R_c , I_c , VISTA Z, Y, J, H, K_s , Johnson-Bessel K and IRAC $3.6\mu\text{m}$, $4.5\mu\text{m}$, $5.8\mu\text{m}$ and $8.0\mu\text{m}$ bands;
- Second panel: SDSS u, g, r, i, z bands;
- Third panel: bands from HST instruments, three UV bands from the WFC3-UVIS ($0.225\mu\text{m}$, $0.275\mu\text{m}$, $0.336\mu\text{m}$), seven optical bands from the ACS-WFC ($0.435\mu\text{m}$, $0.475\mu\text{m}$, $0.606\mu\text{m}$, $0.625\mu\text{m}$, $0.775\mu\text{m}$, $0.814\mu\text{m}$, $0.850\mu\text{m}$) and three near-infrared bands from the WFC3-IR ($1.05\mu\text{m}$, $1.25\mu\text{m}$, $1.60\mu\text{m}$);
- Bottom panel: VIMOS U band, 2 NICMOS near-infrared bands ($1.1\mu\text{m}$ and $1.6\mu\text{m}$) and two WFPC2 bands ($0.30\mu\text{m}$ and $0.45\mu\text{m}$).



Magnitudes and fluxes

Vega Flux Zeropoints

Quantity	U	B	V	R	I	J	H	K	Notes and units
λ_{eff}	0.36	0.438	0.545	0.641	0.798	1.22	1.63	2.19	microns
$\Delta\lambda$	0.06	0.09	0.085	0.15	0.15	0.26	0.29	0.41	microns, UBVRI from Bessell (1990), JHK from AQ
f_{ν}	1.79	4.063	3.636	3.064	2.416	1.589	1.021	0.64	$\times 10^{-20}$ erg cm ⁻² s ⁻¹ Hz ⁻¹ , from Bessell et al. (1998)
f_{λ}	417.5	632	363.1	217.7	112.6	31.47	11.38	3.961	$\times 10^{-11}$ erg cm ⁻² s ⁻¹ A ⁻¹ , from Bessell et al. (1998)
Φ_{λ}	756.1	1392.6	995.5	702.0	452.0	193.1	93.3	43.6	photons cm ⁻² s ⁻¹ A ⁻¹ , calculated from above quantities

These are for the Vega magnitude system and the Bessell et al. (1998) Johnson-Cousins-Glass System.

AB Flux Zeropoints

Quantity	u	g	r	i	z	Notes and units
λ_{eff}	0.356	0.483	0.626	0.767	0.910	microns, from Fukugita et al. (1996)
$\Delta\lambda$	0.0463	0.0988	0.0955	0.1064	0.1248	microns, from Fukugita et al. (1996)
f_{ν}	3631	3631	3631	3.631	3631	Jy or $\times 10^{-23}$ erg cm ⁻² s ⁻¹ Hz ⁻¹
f_{λ}	859.5	466.9	278.0	185.2	131.5	$\times 10^{-11}$ erg cm ⁻² s ⁻¹ A ⁻¹ , calculated from above quantities
Φ_{λ}	1539.3	1134.6	875.4	714.5	602.2	photons cm ⁻² s ⁻¹ A ⁻¹ , calculated from above quantities

These are for the SDSS filters on the AB system. Data from Fukugita et al. (1996) repeat their Table 1, rows 1 and 6.

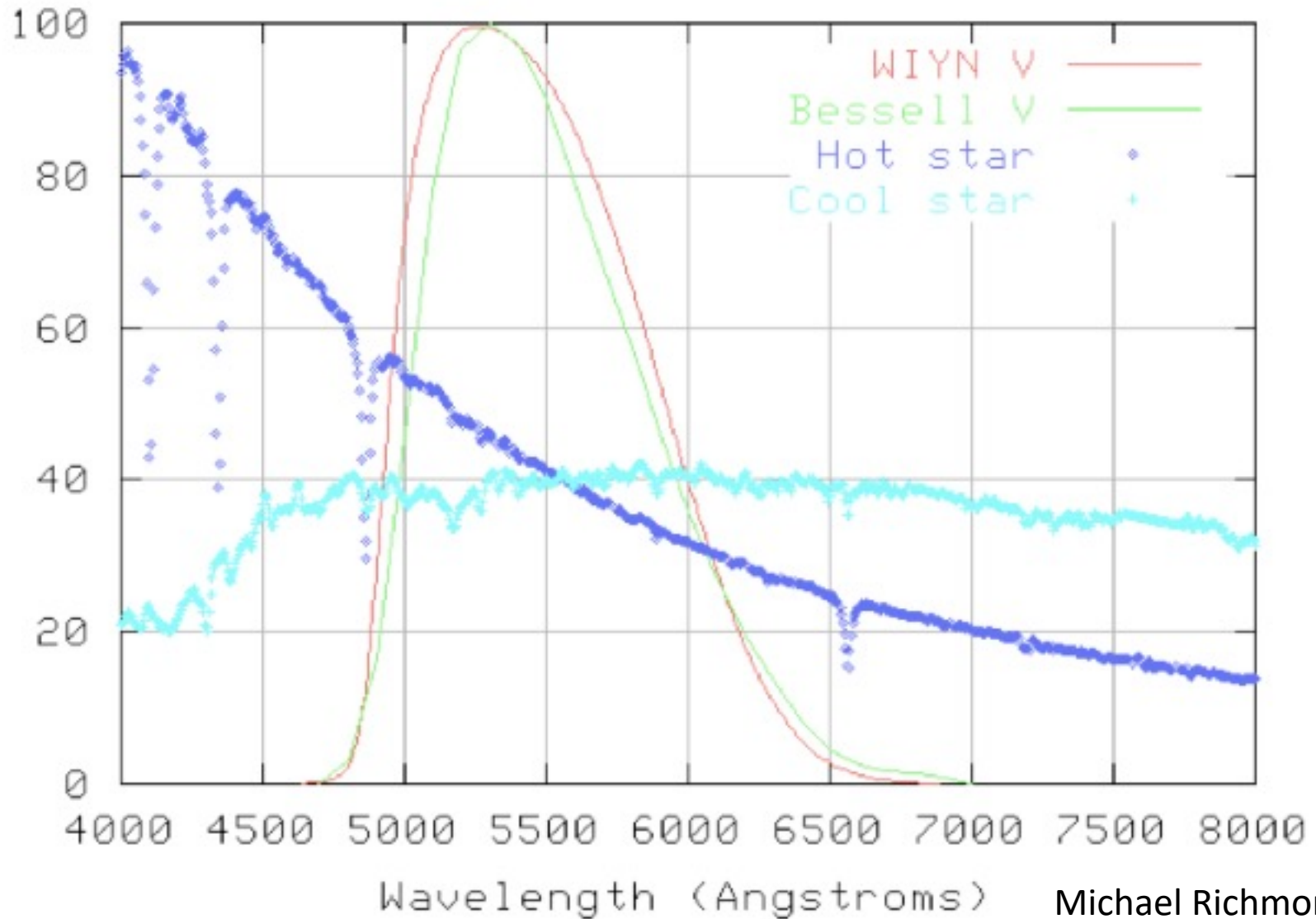
Note that the AB system is defined such that a source with $F_{\text{nu}} = 3.63 \times 10^{-20}$ erg cm⁻² s⁻¹ Hz⁻¹ has AB mag = 0 in every filter, and in general

From <http://www.astronomy.ohio-state.edu/~martini/usefuldata.html>

Filter bandwidth and Transformation

- Wide-band filters have significant colour effects.
 - e.g. in the visible a hot star has decreasing flux with wavelength, whereas it may increase in a cool star.
 - This means that the effective wavelength of the filter depends on the spectrum of the object measured.
- Filters with the same name are not identical
 - Different specifications and manufacturers lead to different bandwidths, transmission profiles
 - Transmission profiles are temperature dependent: they tend to narrow and shift to longer wavelength with decreasing T
 - Big differences can arise if strong, sharp spectral features are included in one passband, but not another
 - Instrument and atmospheric transmission also affects profile
- Need careful calibration to obtain accurate photometric measurements with different instruments

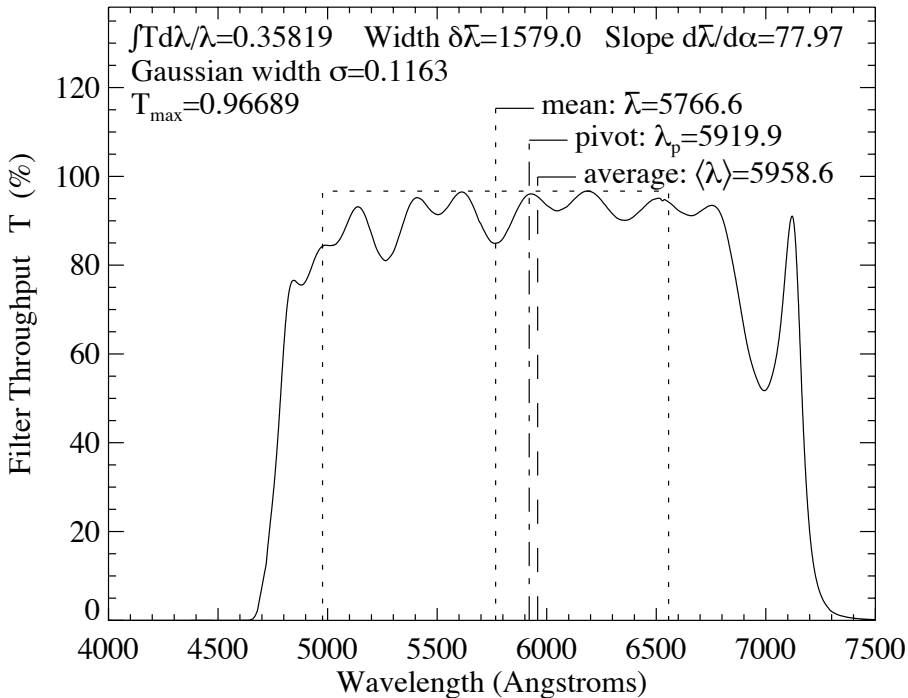
Filter Colour Terms



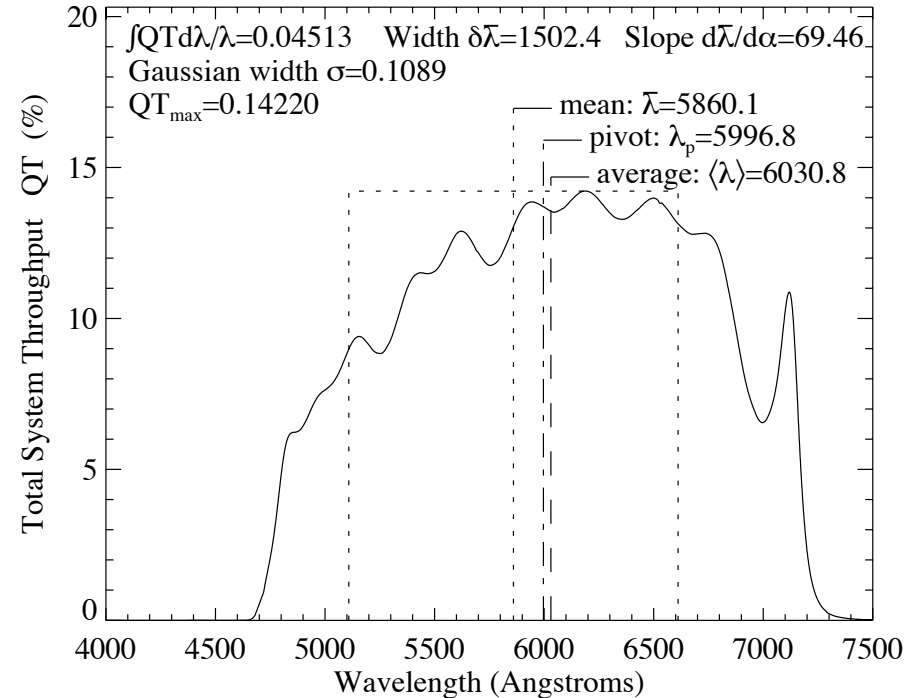
Effects of instrument/Detector Transmission

F606W (Wheel:10 Pos:2)

Filter Throughput T



Total System Throughput QT



Colour transformations have been derived in two ways: one empirically based on UFTI photometry and the other calculated by convolving the known filter profiles with spectroscopic data for a representative set of red stars. The two determinations agree well. The transformations between the old IRCAM3 system and the new MKO-NIR system at H and K are well behaved and single-valued. However, for the J filter different terms have to be applied depending whether or not the standard star has intrinsic water absorption features. This is due to the fact that the new J filter cuts off shorter than the old filter, specifically to avoid water absorption in the terrestrial atmosphere. For stars with no intrinsic water features the colour transformations are:

$$K_{\text{MKO}} = K_{\text{UKIRT}} - 0.020 [+/-0.005] (J-K)_{\text{UKIRT}}$$

$$(J-H)_{\text{MKO}} = 0.960 [+/-0.010] (J-H)_{\text{UKIRT}}$$

$$(H-K)_{\text{MKO}} = 1.205 [+/-0.010] (H-K)_{\text{UKIRT}}$$

$$(J-K)_{\text{MKO}} = 1.040 [+/-0.010] (J-K)_{\text{UKIRT}}$$

However, for stars with significant water absorption, stars with spectral type M4 through to the L class (but not including the T class with methane absorption):

$$K_{\text{MKO}} = K_{\text{UKIRT}} - 0.020 [+/-0.005] (J-K)_{\text{UKIRT}}$$

$$(J-H)_{\text{MKO}} = 0.870 [+/-0.010] (J-H)_{\text{UKIRT}}$$

$$(H-K)_{\text{MKO}} = 1.205 [+/-0.010] (H-K)_{\text{UKIRT}}$$

$$(J-K)_{\text{MKO}} = 0.980 [+/-0.010] (J-K)_{\text{UKIRT}}$$

The UFTI I- and Z-band filters are at significantly longer wavelengths than most optical CCD I and Z filters (with 50% transmission at 0.78 and 0.92 μm and 0.85 and 1.05 μm respectively). The I-band calibration has been compared to Landolt Cousins-I standards (Landolt 1992), and the Z system to the Sloan Sky Survey standards (Krisciunas et al. 1998). The Sloan Z values have been converted from an AB-system to our Vega=0mag system by subtracting 0.572mag from the Krisciunas et al. values. The following transformations were measured :

$$Z_{\text{UFTI}} = Z_{\text{S}} - 0.34 [+/-0.03] (I_{\text{C}} - Z_{\text{S}})$$

$$Z_{\text{UFTI}} = Z_{\text{S}} - 0.21 [+/-0.03] (Z_{\text{S}} - J_{\text{UKIRT}})$$

$$I_{\text{UFTI}} = I_{\text{C}} - 0.72 [+/-0.03] (I_{\text{C}} - Z_{\text{S}})$$

$$I_{\text{UFTI}} = I_{\text{C}} - 0.27 [+/-0.03] (I_{\text{C}} - J_{\text{UKIRT}})$$

The K-Correction

- Central wavelength shifts as a function of z
 - $\Delta\lambda/\lambda = (\lambda_{\text{obs}} - \lambda_{\text{em}})/\lambda_{\text{em}} = z$
- Bandpass stretches as a function of z
- Both effects accounted for in K correction
- No universal relation, related to intrinsic source spectrum
- See e.g. D.W. Hogg et al. 2002, astro-ph/0210394 for definitions and formulae
- Important factors to include when comparing objects at different redshifts – time dilation can also be important for transient events

From CCD frame to photometric data

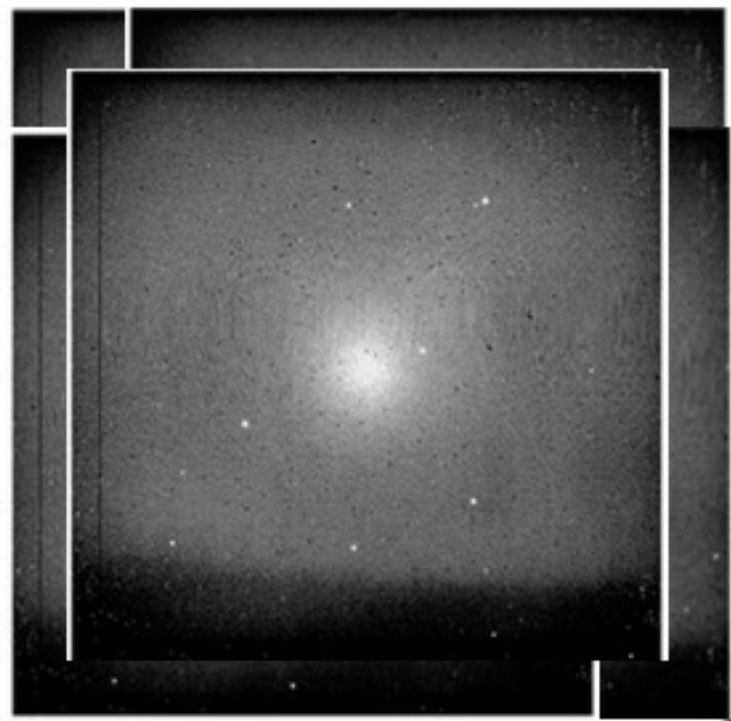
A properly sampled image will have least 2 pixels per FWHM (full width half maximum) of an unresolved stellar image. Note that some instruments undersample the seeing (e.g. VISTA) but then dither or drizzle by fractions of a pixel to improve sampling.

Before extraction of quantitative estimates of the signal, CCD frames must be **bias subtracted, dark count subtracted, corrected for non-linearity and flat field variations and cleaned of cosmic rays** (if necessary). The measured data values also need to be multiplied by the **gain factor** (the number of electrons per adu) to give the correct photon statistics

It is your responsibility to collect the correct frames for data reduction. Do not skimp even though it means you may have less time on-source. Check Data Reduction cookbooks & Instrument manuals

IR Data Reduction

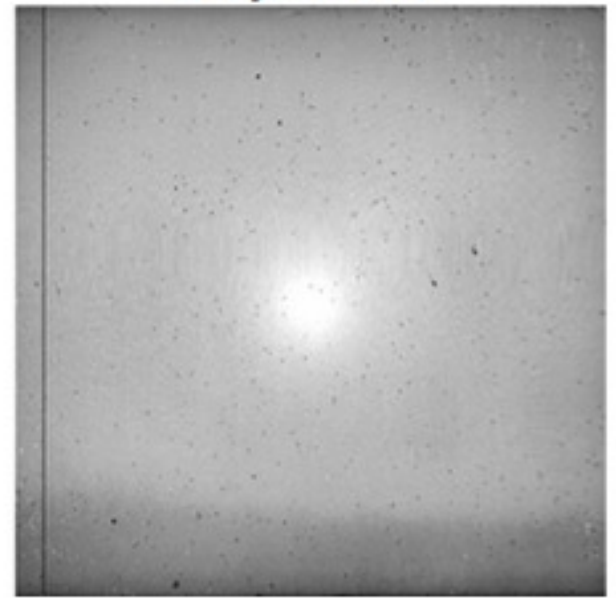
- IR array observations, need more attention to sky background, which is more variable and brighter than at shorter wavelengths
- Typically: obtain a median filtered sky flat from a sequence of images, that have been dithered around the field.
- Multiple observations of science field with small telescope motions in between (dithering) – short exposures are needed because of the bright sky
 - Note that this means that the final image will have a larger field than a the detector format, but that the edges will have less exposure and so greater noise.
- Sky subtraction before flat fielding minimises effects of flat field variations.



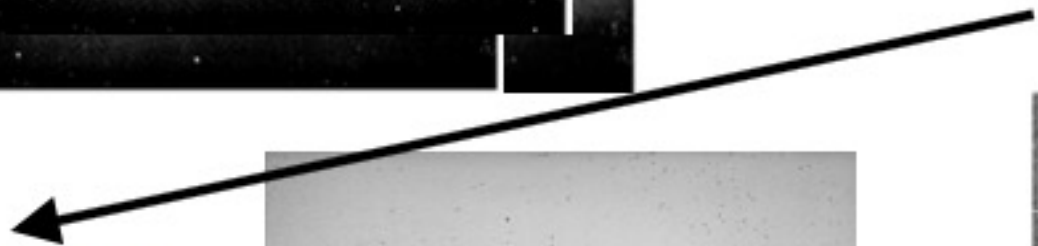
Median



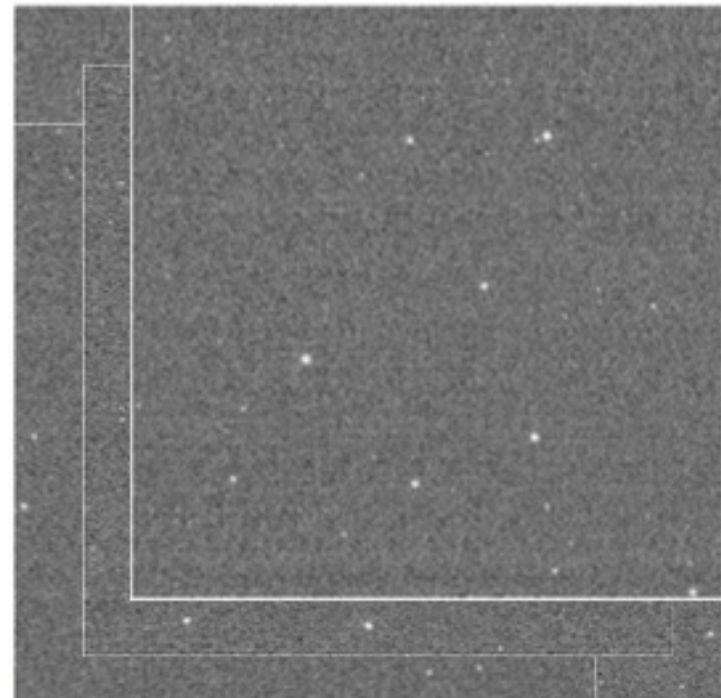
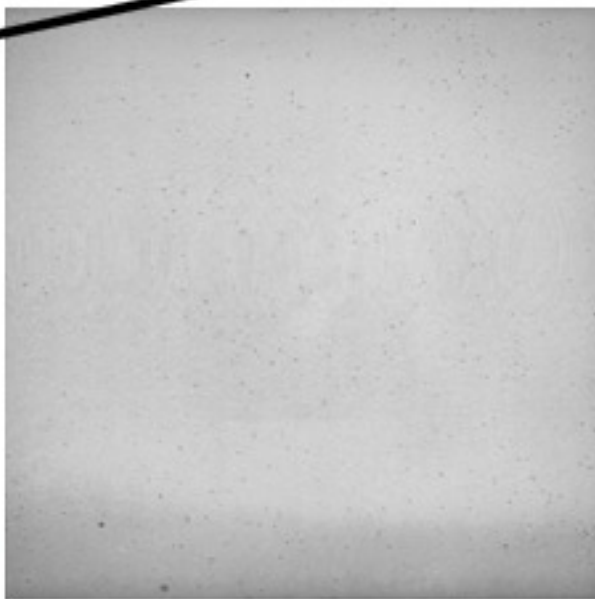
Sky frame



Subtract sky,
divide each by

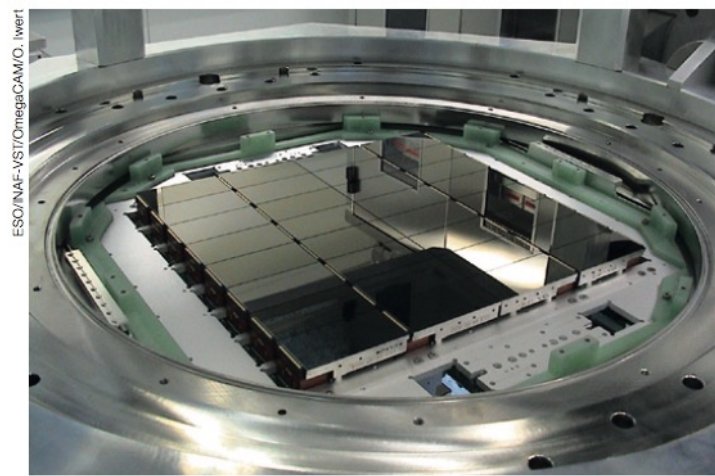


Flatfield

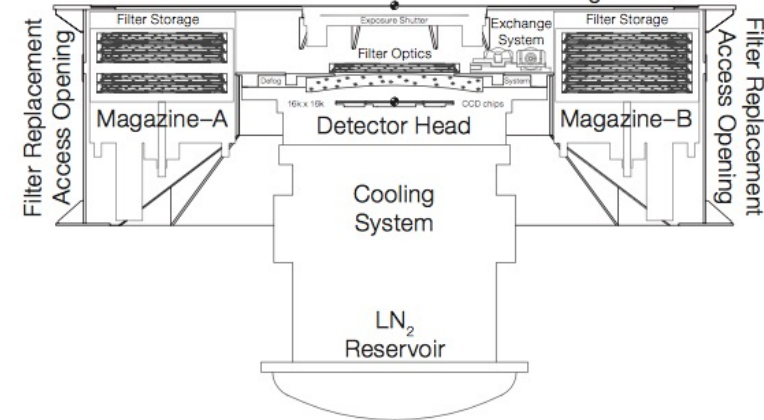


Cameras

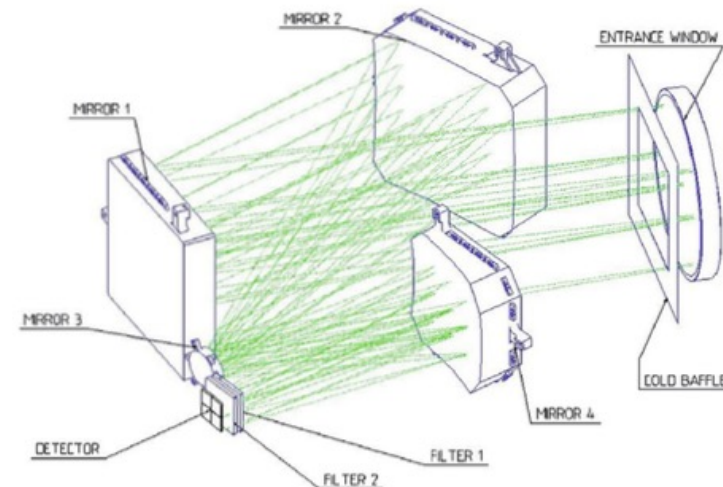
Visible wavelength imagers consist of (a mosaic of) detectors sitting behind a filter wheel in a cryogenic dewar. The 48 CCDs in the OmegaCam/VST camera are shown right.



Infrared instruments usually employ reimaging optics which produce an intermediate image of the telescope pupil to control the background, with the opportunity to deploy filters and other optical elements such as gratings or polarizing prisms near the pupil.



Bottom: the optical layout of the Hawk-I/VLT imager. It samples a 7.5' field at 0.1 arcsec/pixel with 4 x 2k Teledyne HgCdTe detectors. The mirrors image the secondary on to a cold pupil stop at M3 and convert the f/17.5 Nasmyth beam to f/4.4.

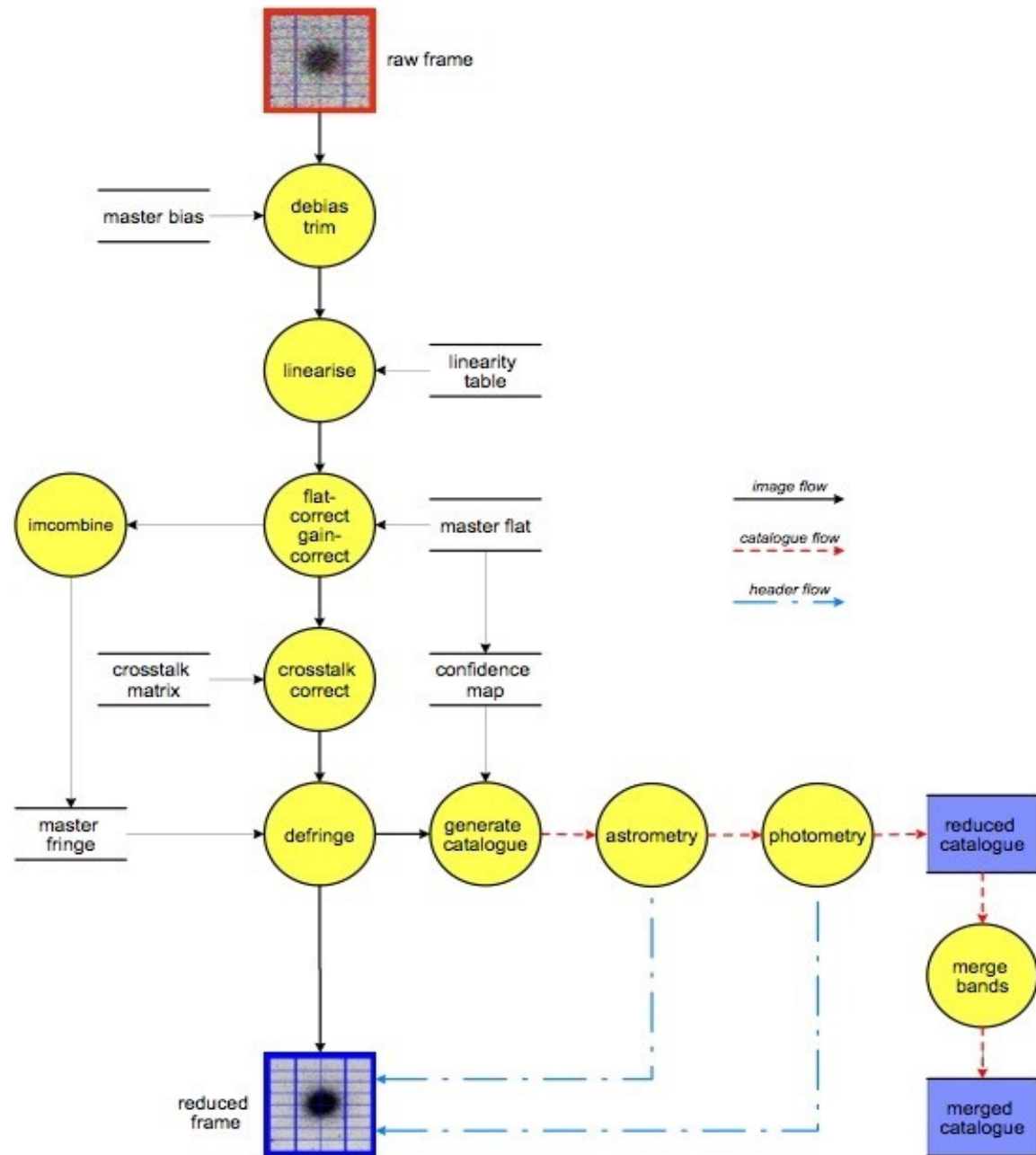


Multi-detector imagers

- Each detector will have its own characteristics - flat field, QE, dark current and operating pixel map etc.
- They will typically also be mounted in slightly different orientations and have different distortions – typically the images at the edge of the field will be more distorted than in the centre
- Accurate photometry or astrometry needs to take these into account
- Most observatories and reduction pipelines take these effects into account, but if you need particularly accurate values, (e.g. for lensing studies) you may need to re- reduce the data.
- Usually offer standard photometric filters + possibly special narrow-band filters for individual spectral features or to isolate emission lines at a particular wavelength.
 - In the IR, generally choose a bandpass between the atmospheric OH lines for lowest background and maximum sensitivity

Cambridge Astronomy Survey Unit

VST survey data
processing and
analysis flow chart



Thermal Backgrounds

At thermal infrared and sub-mm wavelengths, the background signal from emission from the sky and telescope is *much* bigger than the source, and much closer to the instrument

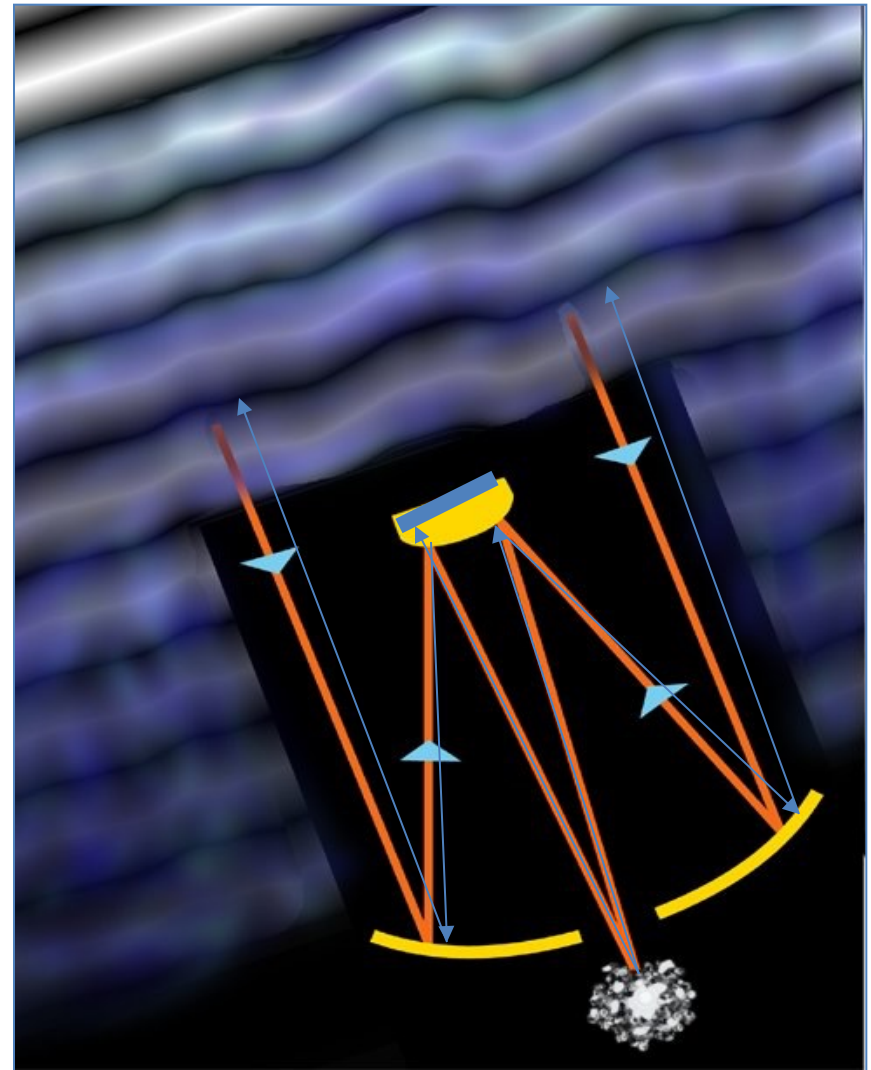
The background is time and position dependent and detectors may suffer from excess $1/f$ noise, so need to measure the background accurately and close in time to the target observations

Generally employ chop-nod or rapid scan techniques to allow differential measurements between the target and the background

Chopping

- The telescope secondary mirror rocks in a quasi-square wave pattern at a few Hz, displacing the image of the object by ~ 20 arcsec on the detector. This allows the weak emission from the astronomical object to be detected differentially on top of the large thermal background
- The mirror position is stabilised with fast guiding at one or both chop positions, ideally chop in azimuth, but reduction will need to account for sky rotation
- Chop throw should be symmetric about the optical axis, and angles should be small so that image quality is maintained ; coma increases as angle increases
- BUT small throws mean that for extended objects, there may be residual flux in the reference position. For extended regions, reconstruction of chopped signals will be needed with consequent increases in observing time and complexity of data reduction and deterioration of S/N.

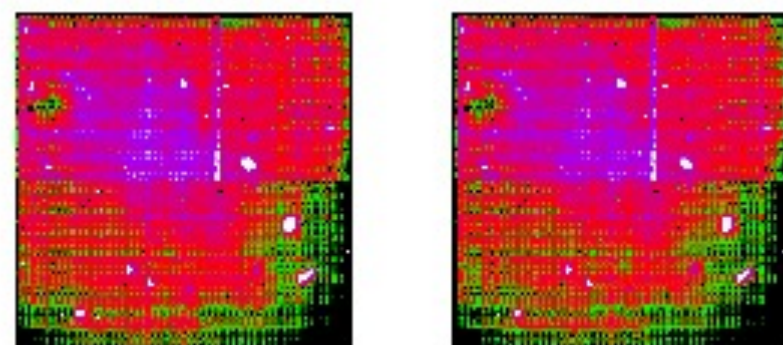
- Big telescopes are better for chopping as the beams separate higher in the atmosphere, and have more overlap on primary mirror
- But large telescopes have larger mirrors and so a greater moment of inertia.
- Focal plane choppers needed on the E-ELT
- E.g. Gemini: chop throw of 20 arcsec corresponds to $\sim 14\text{mm}$ in telescope focal plane
- and a motion of $\sim 11\text{mm}$ on the Primary of diameter of 7.9m
- Secondary mirror is undersized to ensure beam does not spill beyond the coated surface



Chopping and Nodding

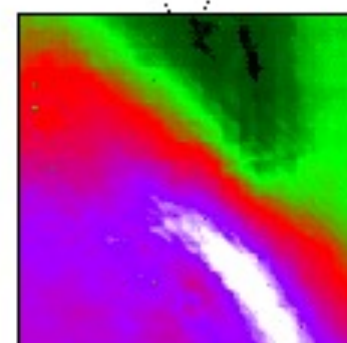
- Motion of secondary mirror, means that the detector beam falls on slightly different parts of the primary mirror, which have different defects, dust etc, leading to a radiative offset between the two chop positions.
- This is compensated by Nodding the telescope so that the object and reference positions are switched.
- Beamswitching :
 - Nod the telescope by a distance equal to the chop throw along the chop axis
- A-B gives net signal corrected for radiative offset
- BUT flexure and temperature changes mean that offset changes with time; observing sequence A,B,B,A removes linear gradient in offset.
- With beamswitching on-chip , final stacked frame has
 - one image with 2 x signal + 2 x sky background
 - two images with 1 x signal + 2 x sky background
 - Coadding all images gives an increase in S/N of $2/\sqrt{3}$ (30% in time)

Nod Position A



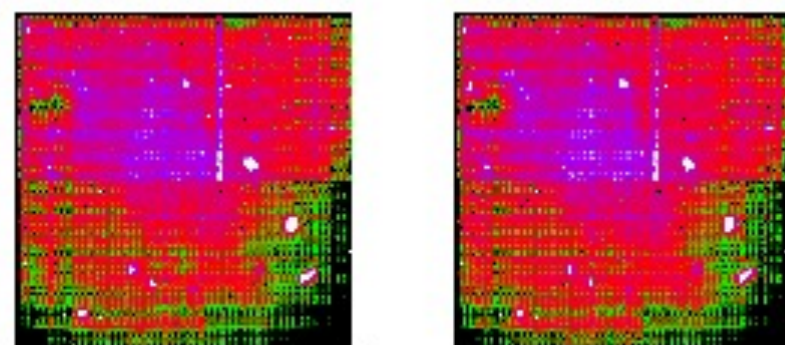
On-Source

Off-Source



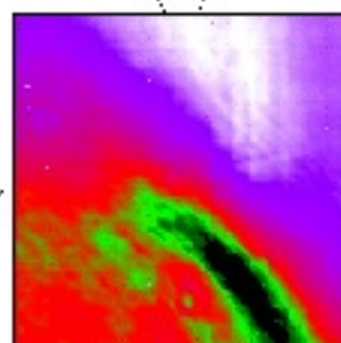
"Chopped Difference"

Nod Position B

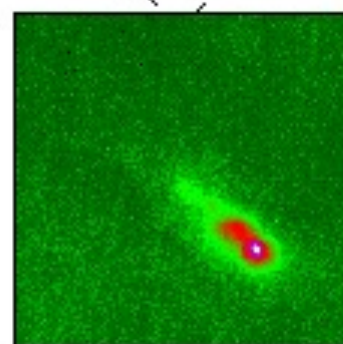


On-Source

Off-Source



"Chopped Difference"



Net Source Signal

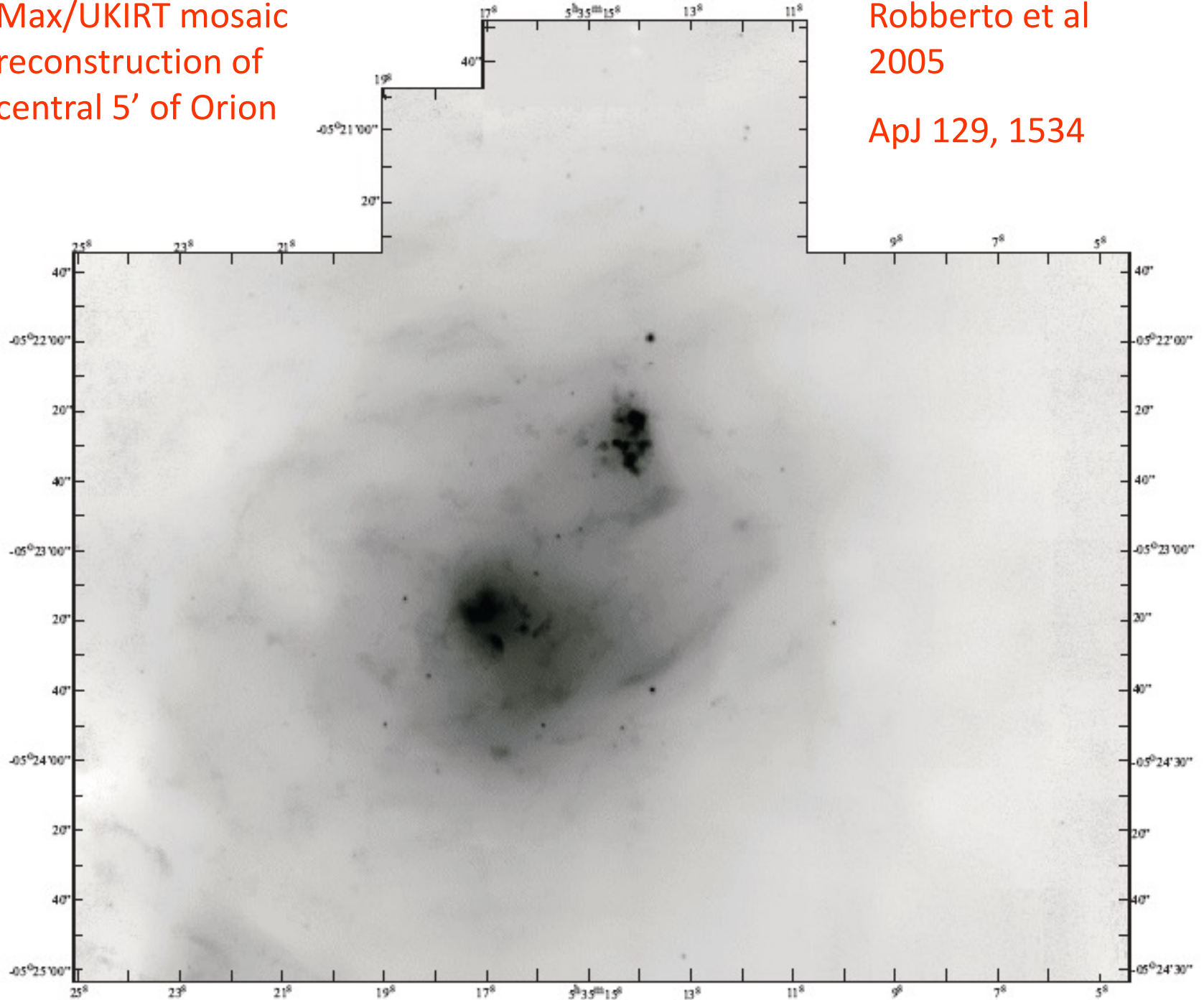
Sensitivity

- BLIP - Background Limited Performance
 - With backgrounds $>10^{10}$ photons/sec/ $\mu\text{m}/\text{m}^2$, should get close to BLIP in all observing modes
 - Requires detector stability and performance, adequate filling of wells, efficient detector read schemes, low electrical noise
 - Theoretical Sensitivity depends on
 - Throughput of atmosphere, telescope & instrument
 - Detector QE (and noise sources - dark and read), read efficiency
 - Emission from sky, telescope and instrument window
 - Telescope efficiency, chop duty cycle, nod settle times, clocking efficiency

Max/UKIRT mosaic
reconstruction of
central 5' of Orion

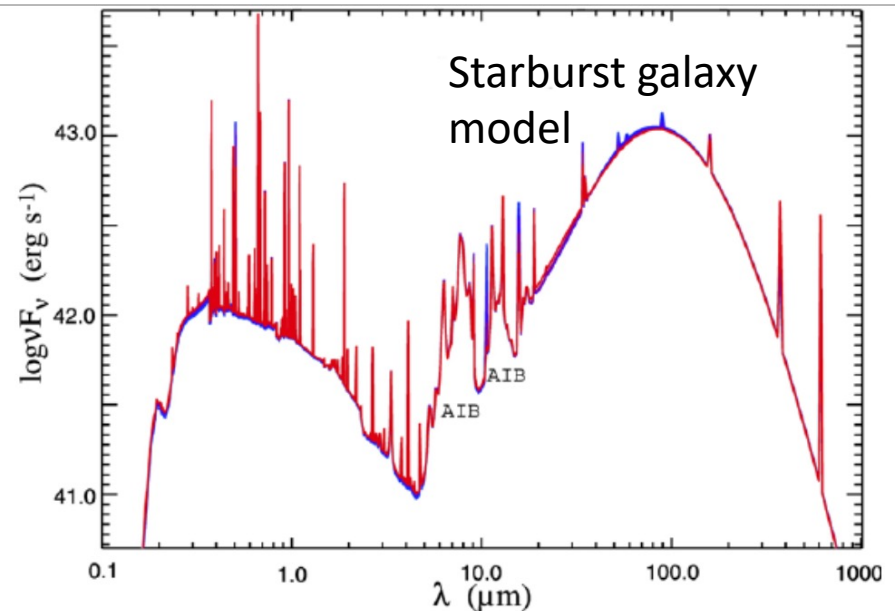
Robberto et al
2005

ApJ 129, 1534



Flux Density and other measures

- Definition of Jansky: $1 \text{ Jy} = 10^{-26} \text{ W m}^{-2} \text{ Hz}^{-1}$
- Radio Continuum normally given in Jy
- But lines may be expressed in K km s^{-1} or
- Antenna temperature
- Spectral energy distributions
in $\text{Wm}^{-2} = \lambda F(\lambda) = \nu S(\nu)$

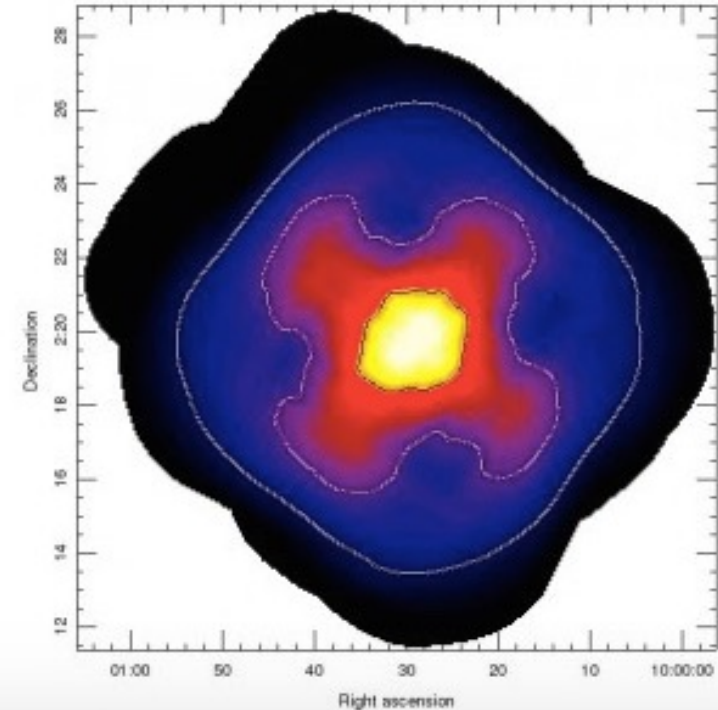
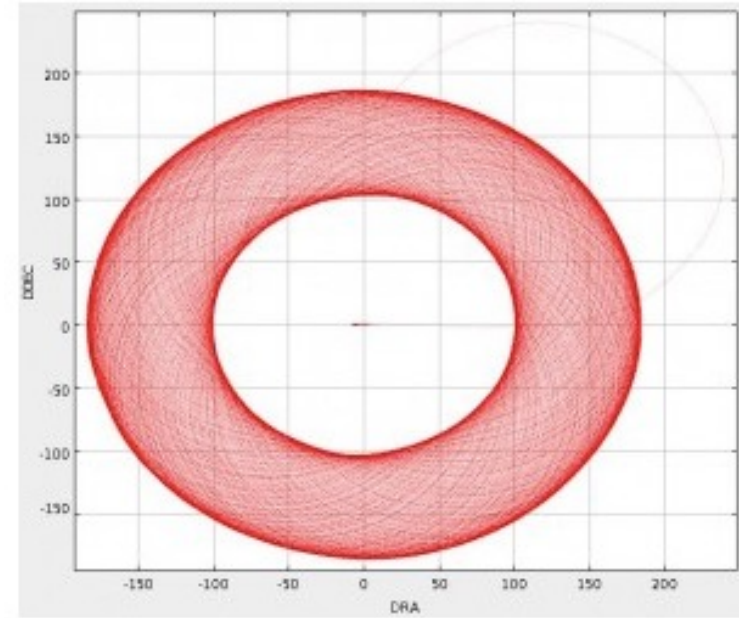


SCUBA-2 Scan Patterns : JCMT

Daisy, constant velocity scans maximise efficiency by eliminating turning points.

The telescope executes a pseudo-circular pattern at a speed of $155''/s$. This pattern keeps the target coordinate on the array throughout the integration and is suitable for compact sources of order 3-arcmin or less, although there is significant exposure time in the map out to 12-arcmin.

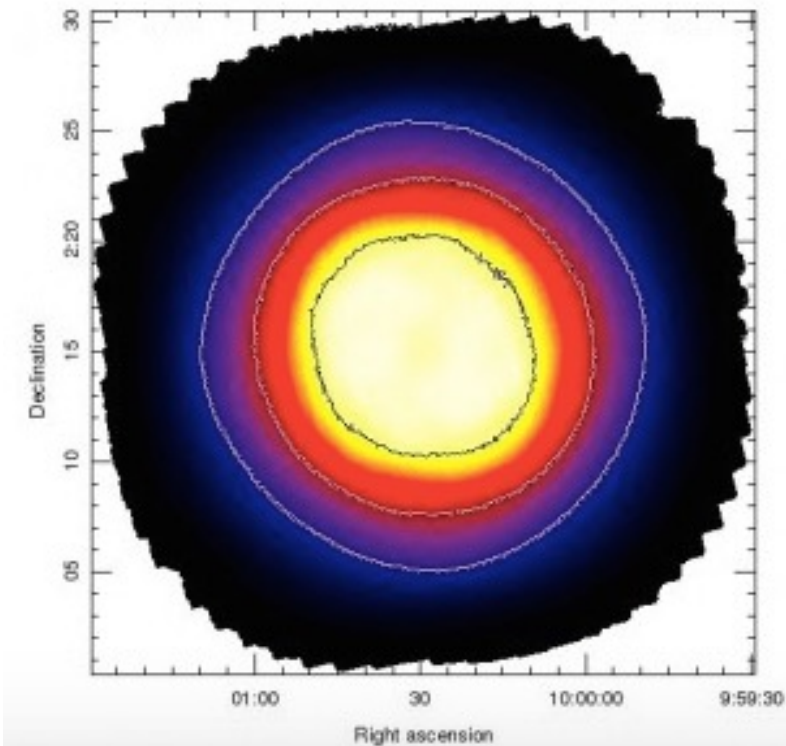
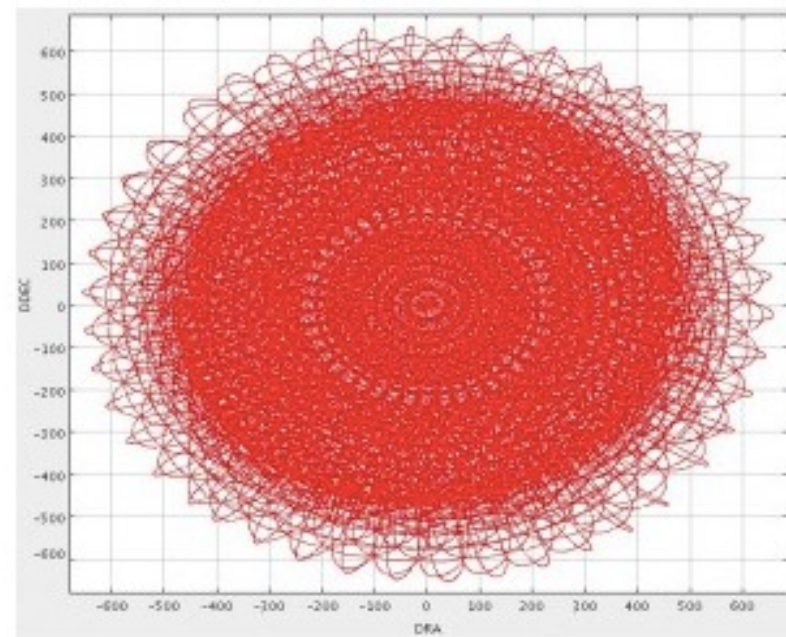
The telescope track for this pattern is shown in the top graph. The exposure time map for a typical observation is shown below, scaled between 0-600 seconds, with contours of 100, 250 and 500 seconds.



SCUBA-2 Scan Patterns : JCMT

15-arcmin Pong map

- The 15-arcmin Pong pattern has a scan spacing of $30''$, telescope velocity of $280''/s$ with 11 rotations of the field ($\sim 8\text{deg}$ apart) within a ~ 40 minute integration.
- The telescope track for this pattern is shown above with the exposure time map for a typical observation below. The image is scaled between 0-160 seconds with contours of 50, 100 and 150 seconds.



<http://www.eaobservatory.org/jcmt/instrumentation/continuum/scuba-2/observing-modes/>

Photometry with Interferometry

- Proceed cautiously!
- Fully processed – ‘Dirty’ - image has many residual structures which inhibit interpretation
- Generally CLEAN algorithm (Högbom 1974) is used to iteratively remove structure arising from the sample pattern in u,v plane of the brightest objects.
 - CLEAN needs intervention for extended objects and does not necessarily conserve flux
 - Can choose the resolution through deconvolution, but may not be sensitive to extended emission which can be distorted
 - Phase errors can redistribute signal within the image

<https://science.nrao.edu/science/meetings/presentation/jdf.webinar.4.pdf>

Interferometric Processing

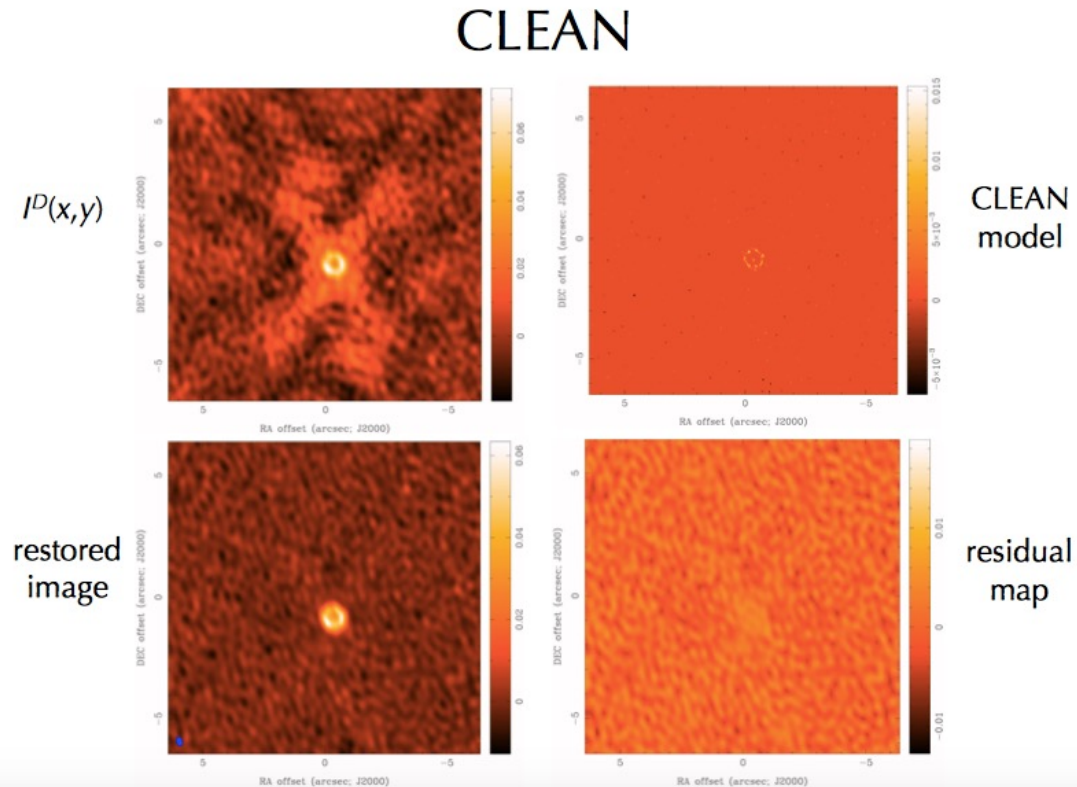
Measures of image quality:

Dynamic range

Fidelity - aliases

Signal-to-Noise ratio

Resolution



Space

In space, there is no need to compensate for the atmosphere!! The background is more stable, but is position dependent – zodiacal light.

Diffraction-limited optics take full advantage of unaberrated wavefronts to yield exquisite, stable image quality and sensitivity

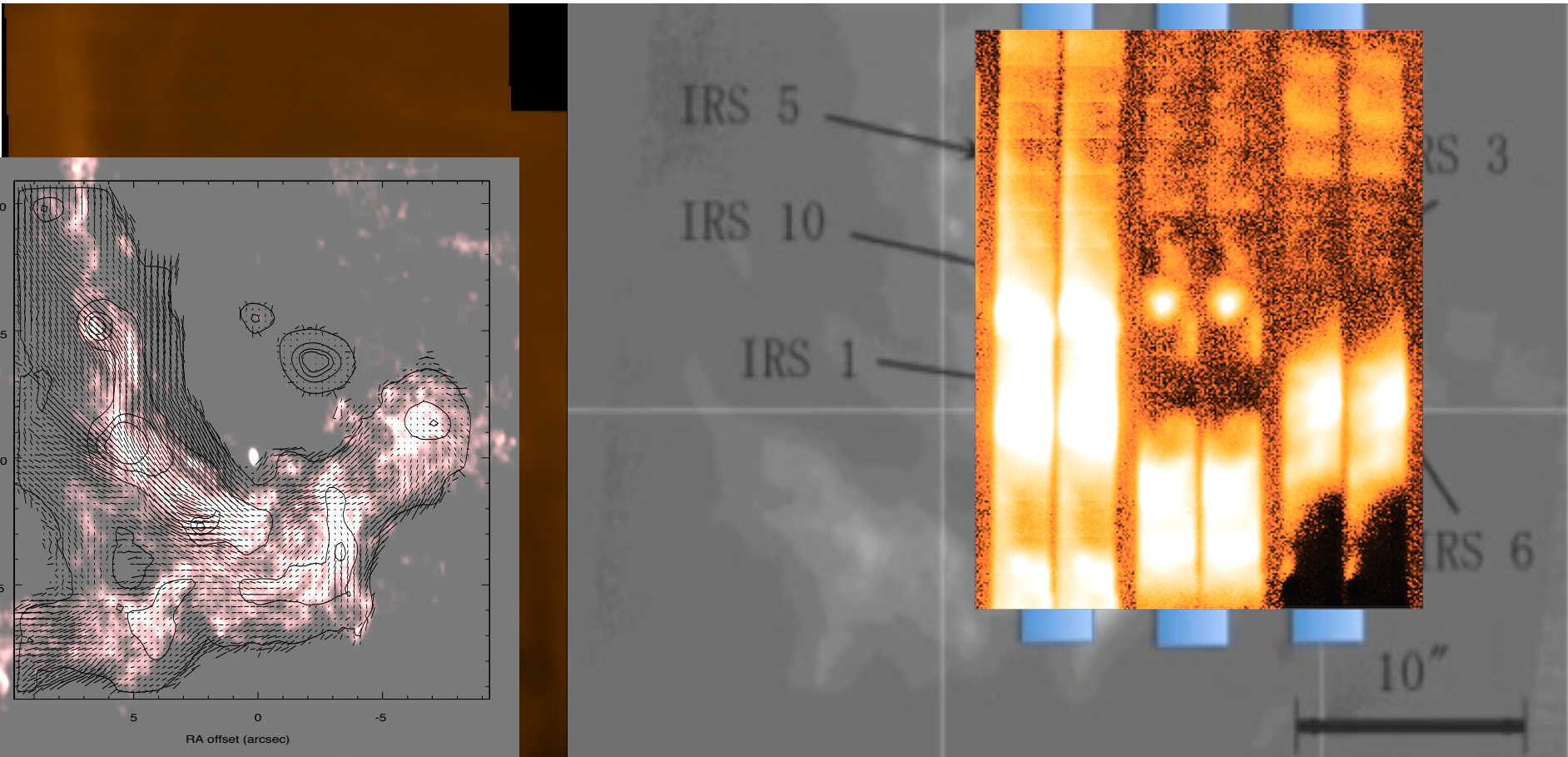
But still have detector characteristics to deal with: cosmic rays, variations in sensitivity across the field of view, changing thermal environments, and possibly image persistence if a bright object has been observed previously.

Radiation damage slowly increases the number of hot pixels and decreases the charge transfer efficiency in CCDs, so it is important to use up-to-date calibration data. There can be jumps in these properties after Coronal Mass ejections.

Polarimetry

- Many objects are partially polarised e.g. via
 - Synchrotron radiation,
 - Scattering in nonsymmetric environments
 - Dichroic emission or absorption
- Radio receivers often split polarization components and measure them directly
- In the visible and IR, polarimetry employs retarders and analysers – e.g. $\lambda/2$ or $\lambda/4$ waveplates in conjunction with a Wollaston or other polarising prism.
- A field mask may be required to separate the images
- Dual-beam Polarimeters measure differentially and so are less sensitive to flat-field errors than photometry

e.g. Canaricam : Galactic Centre

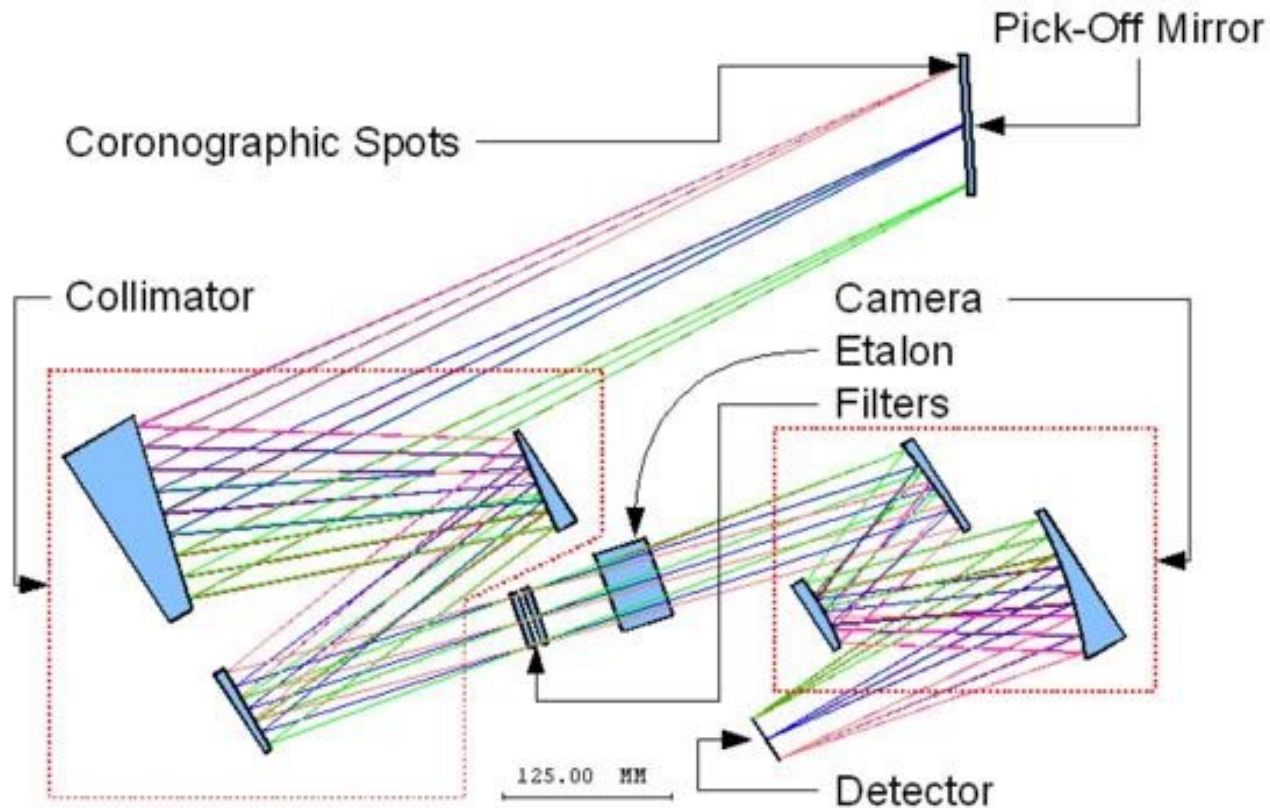


A slit mask in the focal plane provides 3 slots 2×20 arcsc which are transmitted through a Wollaston prism, which separate the e- and o-components of polarization. Rotation of a half-wave plate modulates the polarization signal. The telescope is moved in 1 arcsec steps to fully sample the image.

Tunable Filter Imaging

- A tunable filter can be inserted into the beam to provide narrow-band imaging
 - usually a Fabry-Perot Interferometer, but also Michelson Interferometers, Liquid Crystals etc
 - The transmitted wavelength depends on the angle of the beam through the plates, and so varies across the field, giving rings of constant wavelength centred on the field centre
 - The Plate gap can be scanned to cover sufficient wavelength range to measure a spectral feature over the whole field.

JWST TFI



JWST will have a Tunable Filter imager based on a Fabry-Perot with a set of blocking filters. It operates between 1.5 – 5 μm feeding a 2k HgCdTe detector, and can be used with a coronagraph.

Coronagraphy

Coronagraphs can be used to suppress the light from bright stars or other compact objects.

These can simply be disks inserted into the focal plane, but more effective systems use a combination of focal and pupil plane masks to control the diffraction pattern.

Quadrant Phase Masks and other nulling systems may be effective, providing the telescope tracking is accurate.

The SPHERE instrument on the VLT provides high-strehl AO, differential imaging, spectroscopy and polarimetry with coronagraphy for high contrast observations

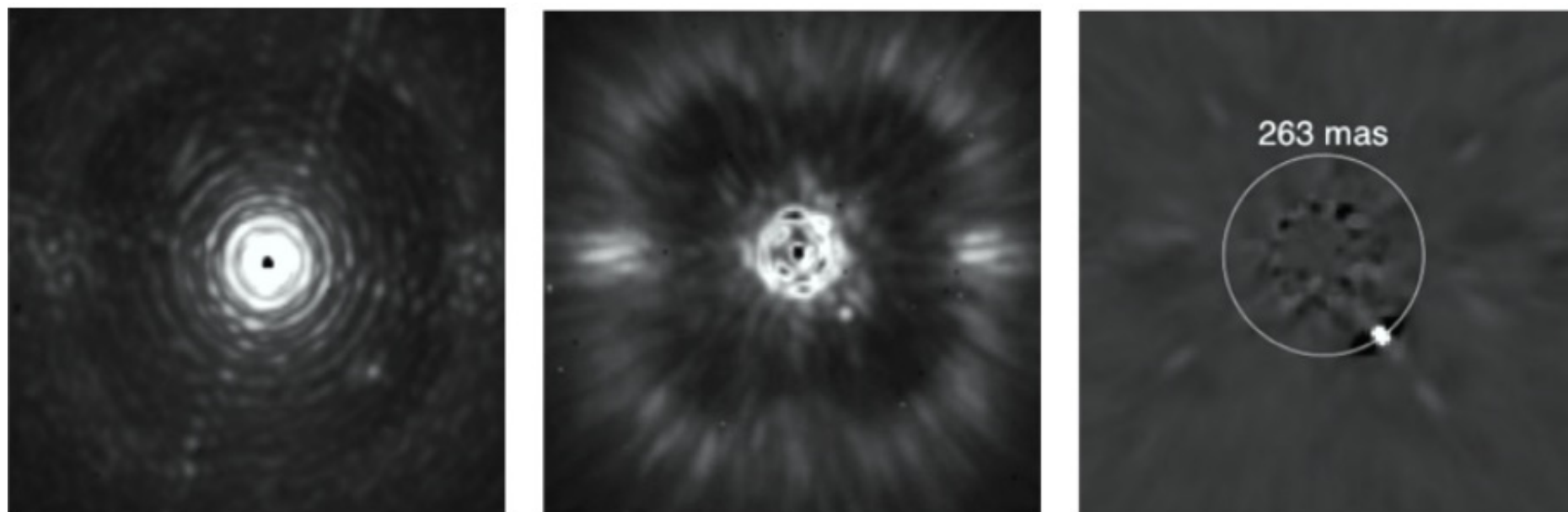
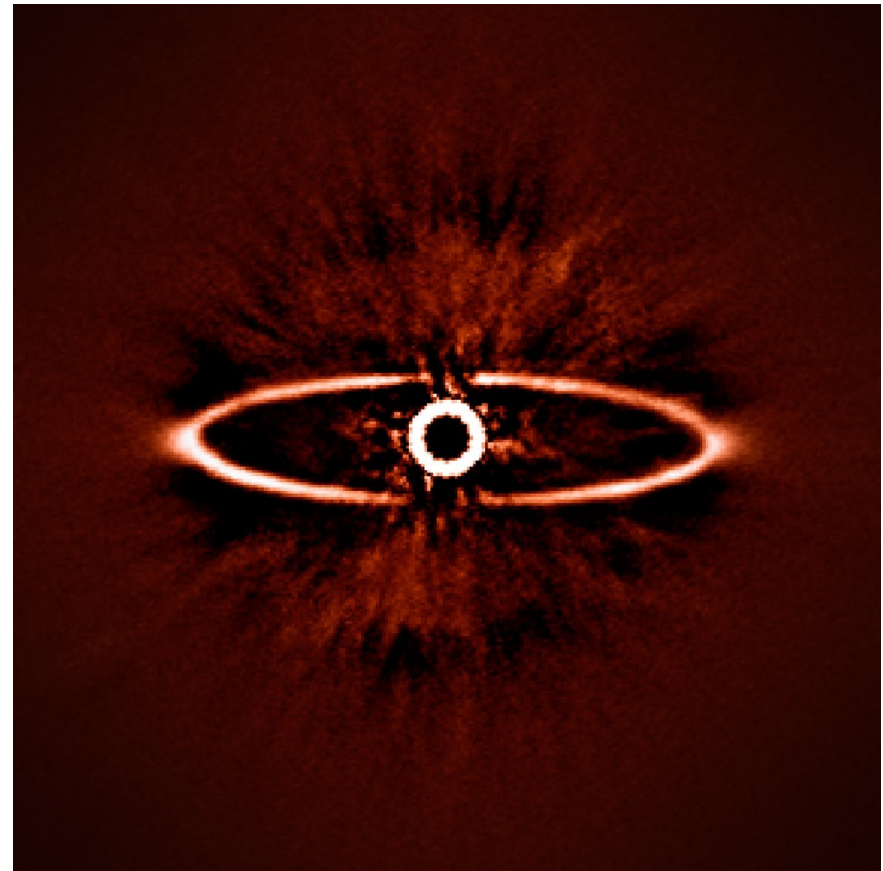
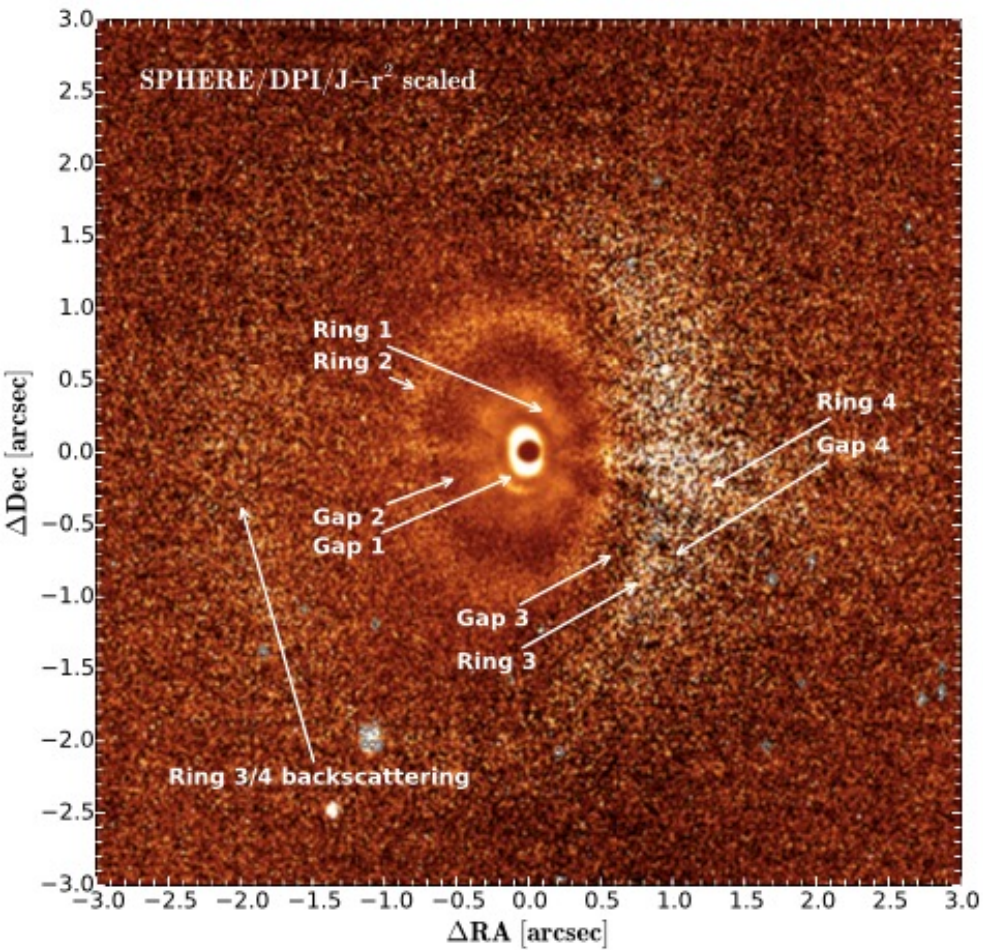


Figure 2: Illustration of the three pillars of high contrast imaging. Left: raw on-sky J-band PSF of SPHERE with IRDIS, showing the diffraction pattern resulting from the almost perfect correction provided by the extreme AO system up to $20 \lambda/D$ in the image (this figure is the number of actuator on the deformable mirror on a side divided by 2). Middle: raw on-sky J-band coronagraphic image of Iota Sgr, illustrating the efficient removal of diffraction rings and pinned speckles by the coronagraph. Note the very visible AO correction radius. Outside the correction radius ($r > 20 \lambda/D$), the brighter halo results from the uncorrected wings of the seeing halo. Right: result of angular differential imaging (ADI) strategy, and post-processing using principal component analysis, cleaning the remaining speckles in the field after extreme AO and coronagraphy, revealing a faint off-axis companion.



VLT/ Sphere images of HD97048 and HR 4796A

Space

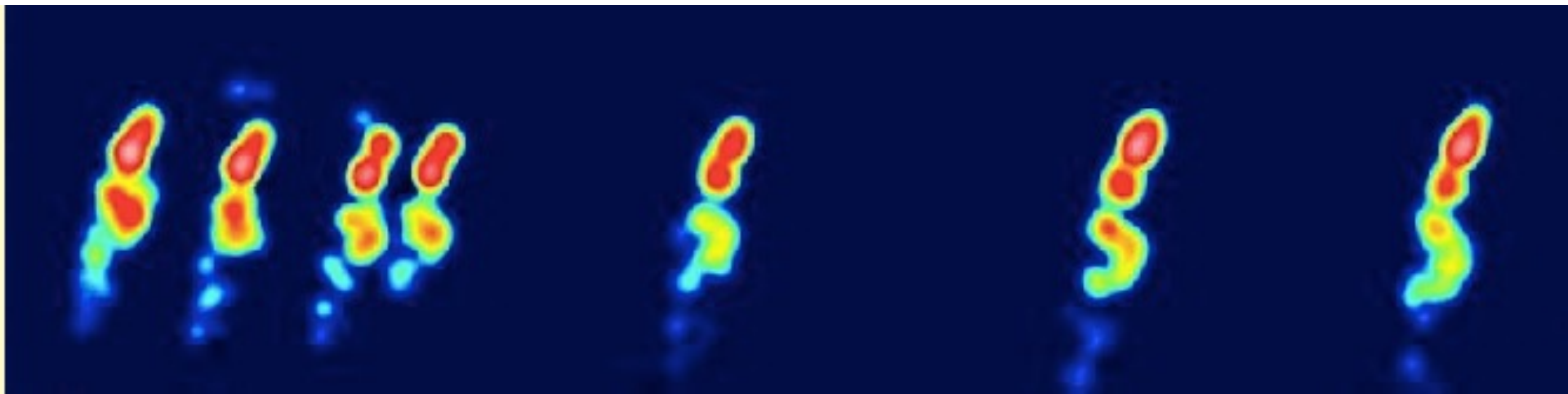
In space, there is no need to compensate for the atmosphere!!

Diffraction-limited optics take full advantage of unaberrated wavefronts to yield exquisite image quality and sensitivity

Interferometry in space can lead to higher resolution through longer baselines

e.g. VLBI using the HALCA satellite extended baselines to 30,000km at 5GHz

Note that the ISM is partially ionized and variations in refractive index can lead to dispersion, scattering and angular broadening at radio frequencies



Multi-epoch 5GHz images of the QSO 1928+738 between 1997 -2001 (DW Murphy)